

Pervaporation Separation of Isopropanol/Benzene Mixtures Using Inorganic–Organic Hybrid Membranes

Junsheng Liu, Yue Ma, Keyan Hu, Hongmei He, Guoquan Shao

Key Laboratory of Membrane Materials & Processes, Department of Chemical and Materials Engineering, Hefei University, Hefei 230022, China

Received 9 September 2009; accepted 20 January 2010

DOI 10.1002/app.32139

Published online 13 April 2010 in Wiley InterScience (www.interscience.wiley.com).

ABSTRACT: A series of pervaporation hybrid membranes were prepared from polyethylene glycol (PEG) and phenylaminomethyl trimethoxysilane (PAMTMS) based on the sol-gel process, in which PEG was used as an organic moiety to improve the affinity for organic alcohols and silicone of PAMTMS was used as inorganic moiety to increase the permeation flux of organic species. Their application to separate isopropanol/benzene mixtures was investigated. FTIR spectra confirmed the reaction products. DSC measurement revealed that the influence of PEG content on the T_g and thermal behavior of membranes A, B, and C. FE-SEM images exhibited that phase-separated structure has occurred when the PEG content elevated to some extent. Pervaporation experiments showed that the permeation flux increased and the separation factor decreased with an increase in isopropanol

(IPA) content in feed at 30°C. Meanwhile, the separation factor increased with an increase in feed temperature at 60 vol % IPA content. Moreover, it was found that the permeation flux was independent of the feed temperature, suggesting that feed temperature has little impact on the thermal motion of polymer chains. The increasing cross-linking degree in hybrid matrix might be responsible for such trend. Based on these findings, it can be concluded that these pervaporation hybrid membranes have potential applications in the separation of isopropanol/benzene binary mixtures. © 2010 Wiley Periodicals, Inc. *J Appl Polym Sci* 117: 2464–2471, 2010

Key words: hybrid membrane; pervaporation; sol-gel process; isopropanol/benzene mixtures; close-boiling point liquid mixtures

INTRODUCTION

Pervaporation (PV) is considered as one promising process for the separation of close-boiling point liquid mixtures, azeotropic or temperature-sensitive species that are currently difficult to be separated by the conventional azeotropic or extractive distillation, which is the reason why PV separation technique attracts such high interest in recent years.^{1–5}

It is well known that PV is mainly dependent on the selectivity of membranes toward different kinds of components of liquid mixture. Thus, the selectivity and separation performances of the membranes used are the major consideration for separating organic/organic mixtures or organic/water solution.^{6,7} For such purpose, various innovative techniques are newly developed. Among these, inorganic/organic

hybrid is considered as one of the most effective methods to improve the permeation flux and selectivity of PV membranes.^{7–11} For example, Ohshima et al.⁷ prepared a series of organic/inorganic hybrid membranes for the removal of 0.05 wt % benzene/water mixed solution, and found that hybridization of organic and inorganic moieties can increase the membrane selectivity. Zhang et al.⁸ prepared the PVA/APTEOS hybrid membranes for the separation of ethanol/water mixtures, and found that the trade-off between the permeation flux and water permselectivity could be effectively resolved by the incorporation of inorganic silica. In addition, Kulkarni et al.¹¹ prepared the PVA/TEOS hybrid membranes to separate water–isopropanol mixtures, and found that the membrane containing 1.5 : 1 mass ratio of TEOS to PVA gave the highest separation selectivity of 900 at 30°C for 10 mass percentage of water in the feed mixture.

However, the current researches primarily focus on the removal of water from organic/water solution, few attempt is made to separate organic/organic mixtures using inorganic/organic hybrid membranes by PV technique. These previous studies are thus unsatisfactory, further work is still necessary.

As one type of alcohol/benzene extractives, isopropanol (IPA), and benzene (Bz) are typical close-

Correspondence to: J. Liu (jsliu@hfuu.edu.cn) or K. Hu (kyhu@hfuu.edu.cn).

Contract grant sponsor: Anhui Provincial Natural Science Foundation; contract grant number: 090415211.

Contract grant sponsor: Significant and General Foundations of Educational Committee of Anhui Province; contract grant numbers: ZD2008002-1, KJ2008B007.

TABLE I
Physical Properties of Isopropanol and Benzene

Entry	Isopropanol ^a	Benzene ^a
Formula weight	60.1	78.11
Density (g/mL, °C)	0.7855	0.8787
Melting point (°C)	-89.5	5.5
Boiling point (°C, 760 mm Hg)	82.4	80.0
Heat capacity (J deg ⁻¹ mol ⁻¹)	155.0	136.0

^a These data were extracted from Ref. 12.

boiling point compounds and widely used in industry as solvent or extracting solvent for azeotropic distillation (physical properties of isopropanol and benzene¹² are listed in Table I). Because of the tiny difference of boiling point, isopropanol/benzene mixtures are hard to be separated by conventional distillation apparatus, thus it is a big challenge to separate isopropanol/benzene mixtures. Hopefully, PV technique makes such separation become promising.

Recently, some efforts were made to prepare and characterize inorganic/organic hybrid membranes.^{13–17} In these articles, a series of novel inorganic/organic hybrid membranes were successfully synthesized via sol-gel process, revealing that both the thermal stabilities and separation performances of these hybrid membranes were highly improved. It is hoped that these hybrid membranes can also be used to separate close-boiling point or azeotropic mixtures by PV technique.

Therefore, to expand the applications of inorganic/organic hybrid membranes in some new fields, such as the separation/recovery of organic-organic mixtures, herein, a series of pervaporation hybrid membranes are prepared from polyethylene glycol (PEG) and phenylaminomethyl trimethoxysilane (PAMTMS) based on the sol-gel process. Compared with the previous articles,¹⁷ special attention is paid to the preparation of PAMTMS/PEG hybrid membranes using PEG as an organic moiety to improve the affinity of hybrid membranes for organic alcohols, and silicone of PAMTMS as inorganic moiety to increase the permeation flux of organic species. Moreover, the effects of IPA content in feed and feed temperature on the PV properties of the hybrid membranes produced are also evaluated.

EXPERIMENTAL

Materials

Phenylaminomethyl trimethoxysilane (PAMTMS, purity: $\geq 95.0\%$) was purchased from Silicone New Material Co. Wuhan University (Wuhan, China) and used without further purification. Polyethylene glycol (PEG) ($M_n = 1000$), dimethyl formamide (DMF), benzene (Bz, purity: $\geq 99.5\%$), and isopropanol (IPA,

purity: $\geq 99.5\%$) were purchased from Shanghai Chemical Reagent Co. (Shanghai, China) and used as received. Other reagents were of analytical grade and used as received.

Membrane preparation

Pervaporation hybrid membranes A, B, and C used in this case were prepared from PEG and PAMTMS based on sol-gel process, the molar ratio of PEG and PAMTMS for preparing these membranes is listed in Table II. The procedure steps can be briefly described as follows:

First, PAMTMS (10 mL) was dissolved in DMF solution (20 mL) and stirred for 1 h at room temperature. Subsequently, the prescribed amount of PEG dissolved with deionized water at room temperature was added dropwise into the PAMTMS and DMF mixed solution; after the mixture was stirred violently for 10 h, a light-yellow hybrid precursor could thus be achieved.

To develop a pervaporation hybrid membrane, the above-prepared hybrid precursor was cast on a teflon plate and dried at 80°C for 24 h to remove the solvent, and then cooled down to room temperature. This step might be repeated several times so as to increase the thickness of the prepared membrane. The final pervaporation hybrid membrane could thus be obtained.

Sample characterizations

Fourier transform infrared (FTIR) spectra of the products were obtained using a Shimadzu FTIR-8400S Fourier transform infrared spectrometer in the region of 4000–400 cm⁻¹ with a resolution of 0.85 cm⁻¹.

Differential scanning calorimetry (DSC) measurement was carried out on a Shimadzu DSC-60 equipment at a heating rate of 10°C min⁻¹, in an atmosphere of dry nitrogen.

FE-SEM images were observed using field-emission scanning electron microscopy (FE-SEM) (Sirion 200), operated with an accelerating voltage of 5.00 kV.

Pervaporation measurements

Pervaporation experiments were conducted using a pervaporation separation setup (see Figure 1,

TABLE II
The Molar Ratio of PAMTMS and PEG in Hybrid Membranes A, B, and C

Membrane number	PAMTMS (mol)	PEG (mol)
A	0.1	0.01
B	0.1	0.02
C	0.1	0.03

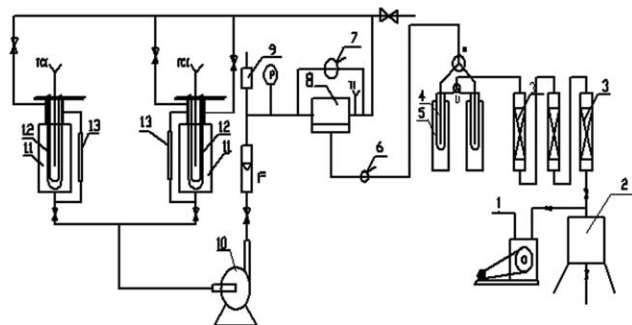


Figure 1 The pervaporation separation setup. 1-Vacuum pump, 2 and 9-Buffer, 3-Desiccator, 4- U-tube collector, 5- Cold trap, 6- Pressure transmitter, 7- Differential pressure indicator, 8-Membrane cell, 10-Feed circulator, 11-Feed container, 12- Heater, 13-Liquid level indicator; F-Flow meter, TCI-Thermocouple indicator, TI-Temperature indicator.

Beiyang Chemical Corporation of Tianjin University, China), at feed temperature range of 30–60°C, and IPA content in feed range of 20–80 vol %. The effective membrane area was 16 cm² and the feed flow-rate was controlled at 10 L min⁻¹. The thickness of membranes was around 110 μm. The vacuum in the permeate side was maintained at 0.1 MPa using a vacuum pump, and the penetrant was collected in a cold trap. The content of feed solution and penetrant were determined using a gas chromatograph equipped with a flame ionization detector (FID) and capillary column (SP-2100A, Beijing, China). The membrane PV performances of permeation flux (J_p , g/m²h), and separation factor (α) can be calculated from Eqs. (1) and (2)¹⁸:

$$J_p = \frac{W}{A \times t} \quad (1)$$

$$\alpha = \frac{P_{IPA}/P_{Bz}}{F_{IPA}/F_{Bz}} \quad (2)$$

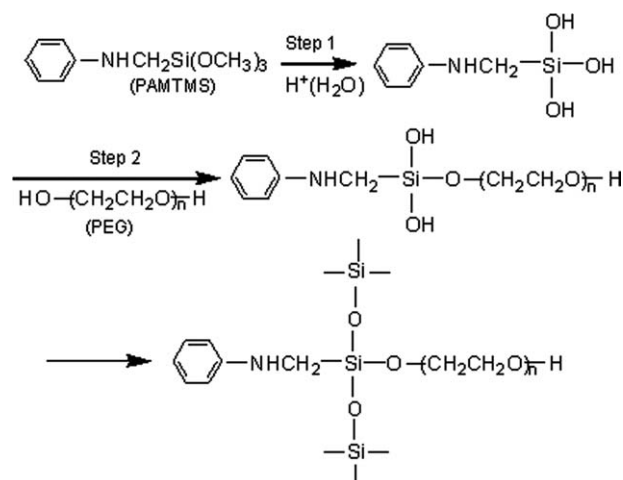
where W is the weight of the penetrant collected (g) in permeation time t (min), and A is the effective membrane area (m²). P and F are the weight fractions in the penetrant and feed solution, respectively. The subscripts of IPA and Bz denote the isopropanol and benzene, respectively.

RESULTS AND DISCUSSION

FTIR spectra

As shown in Scheme 1, the preparation of pervaporation hybrid membranes included two steps: i.e., the hydrolysis and polycondensation of Si—OH in PAMTMS with —OH in PEG molecular chains to form the Si—O—Si bonds in the hybrid matrix.

To demonstrate the reaction products, FTIR spectroscopy was conducted and shown in Figure 2. As



Scheme 1 The sol-gel process for the preparation of hybrid membranes, step 1 is the hydrolysis of PAMTMS, steps 2 is the polycondensation of hybrid precursor to create Si—O—Si bonds in the hybrid matrix.

typical examples, only the FTIR spectra of samples B and C are presented.

As shown in curve (a), the strong absorption peak at 1108 cm⁻¹ is the overlapping of the asymmetric stretching of Si—O—Si with Si—O—C, C—O—C stretching bands in hybrid membrane B.^{19,20} The distinct absorption peaks associated with —CH₃ or —CH₂— groups are observed at 2920 cm⁻¹. The peak located at near 3444 cm⁻¹ is ascribed to N—H bond, and the peak at 1410 cm⁻¹ is in the range of 1220–1500 cm⁻¹ assigned to the C—N stretching vibration.¹⁷ The peak at 748, 690, and 1632 cm⁻¹ can be ascribed to the phenyl group in the molecular chains. The peak at 2368 cm⁻¹ is the vibration of C—O bond from PEG moiety.²¹

By comparison curve (b) with curve (a), it can be noted that the curve shape of FTIR spectra is very similar except that two peaks centered at 1108 and

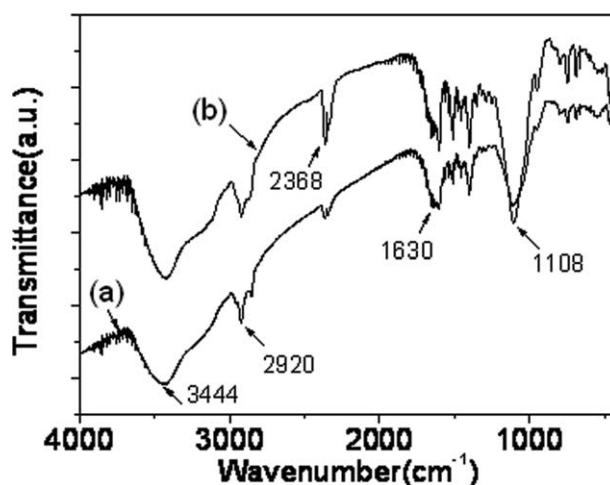


Figure 2 The FTIR spectra of (a) and (b) is the membranes (B) and (C), respectively.

TABLE III
Solubility of Hybrid membranes A, B, and C in Different Organic Solvents

Solvent	PAMTMS	Hybrid precursor	Hybrid membrane
Methanol	S ^a	S	S
Ethanol	S	S	S
Isopropanol	S	S	I ^b
n-Butanol	S	S	S
DMF	S	S	S
Chloroform	S	S	S
Dichloromethane	S	S	S
Benzene	S	S	I

^a S indicates soluble.

^b I means insoluble.

2368 cm⁻¹ have become much steeper when PEG content was increased (cf. Table II). The reason can be assigned to the increasing PEG in the hybrid matrix, resulting in an increase in the peak intensity of C—O vibration. These changes in adsorption peaks corroborate the reactions presented in Scheme 1.

Solubility in organic solvents

For PV separation of organic–organic mixtures, solubility of a hybrid membrane in organic species is of great importance and needs to be considered seriously, in that these organic mixtures may hurt the hybrid membrane and decrease its stability.⁷ Thus, the solubility of hybrid membranes A, B, and C, and the related silicone PAMTMS, hybrid precursor in various organic solvents are measured and tabulated in Table III.

It can be seen that both PAMTMS and hybrid precursor are soluble in the tested organic solvents. Meanwhile, the pervaporation hybrid membranes prepared from these hybrid precursors also have excellent solubility in most organic solvents. However, it is interesting to find that they are insoluble in both isopropanol and benzene. Isopropanol/benzene mixtures are therefore selected as separation media for the measurements of PV performances of hybrid membranes A, B, and C.

DSC measurement

Inspecting glass transition temperature (T_g) of the hybrid membranes produced will favor the recogni-

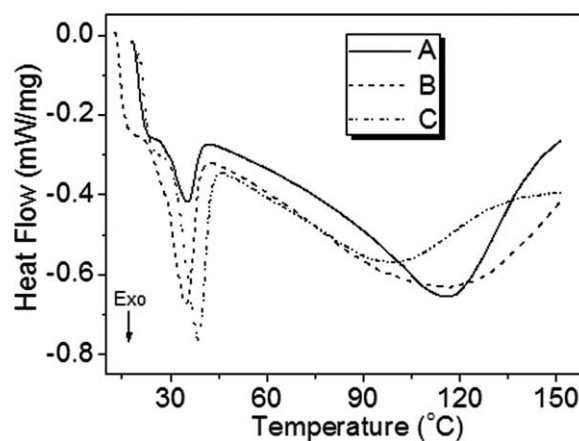


Figure 3 DSC curves for membranes A, B, and C.

tion of crystallization transformation from rigid to flexible. DSC measurement was thus conducted and the DSC curves are presented in Figure 3.

As shown in Figure 3, it can be found that the T_g is 24.79, 19.79, and 25.54°C for membranes A, B, and C, respectively. Meanwhile, it can also be found that there exist two exothermic and one endothermic peaks in the DSC curves and the enthalpy of transition (ΔH) is listed in Table IV. It is reported²² that in DSC curves, the single or multiple endothermic peaks are the crystal melting, whereas the exothermic peak can be considered as the crystallization. Consequently, for membranes A, B, and C, the crystallization temperature (T_c) is positioned at around 35.29, 34.85, and 38.60°C, suggesting an amorphous to crystalline form. Whereas, the melting point temperature (T_m) is near at 41.95, 42.40, and 46.17°C, which was elevated as the PEG content increases. The upward trend in T_m can be ascribed to an increase in the branching chain and cross-linking degree in the hybrid network because of more PEG being incorporated into the hybrid membranes.

Furthermore, by comparing the T_g with T_c , it can be seen that they reveal the same change trend: i.e., membrane B indicates the lowest value. The reason can be assigned to the change of thermal transition behavior when the PEG content in membranes A, B, and C increases. As stated, the lower the PEG content in hybrids, the more perfect the silica network, and the higher the T_g of PEG embedded in

TABLE IV
DSC Data of the Prepared Membranes A, B, and C

Sample	T_g (°C)	First thermal degradation peak				ΔH (J/g)	Second thermal degradation peak			
		Position (°C)			ΔH (J/g)		Position (°C)			ΔH (J/g)
		Onset	Peak	Endset			Onset	Peak	Endset	
A	24.79	28.87	35.29	39.26	-7.41	69.12	116.02	143.83	-132.73	
B	19.79	27.50	34.85	38.98	-21.78	51.72	116.51	151.21	-107.02	
C	25.54	31.44	38.60	42.44	-21.65	52.10	98.97	133.76	-69.10	

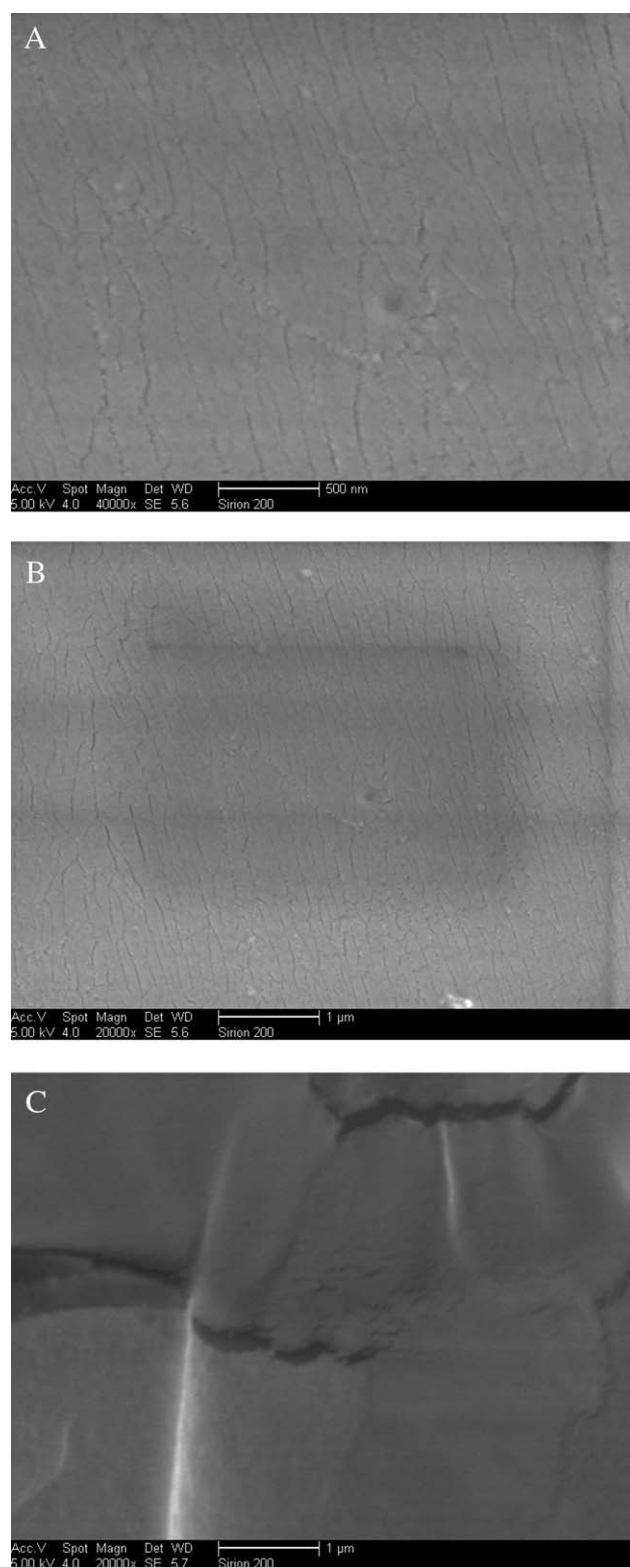


Figure 4 FE-SEM images of membranes A, B, and C.

hybrids.²³ Moreover, the phase-separated structure between the inorganic and organic moieties²⁴(cf. FE-SEM images in Figure 4(c), hereinafter) will also affect the T_g , T_c , and T_m of these membranes. As for membrane B, its lower T_g and T_c might be related to

its lower crosslinking degree as confirmed by the relative lower permeation activation energy (cf. Table V, hereinafter).

The above findings clearly demonstrate that PEG content in membranes A, B, and C has some influences on their crystallization temperature and thermal transition behavior.

FE-SEM images

Figure 4 presented the FE-SEM images obtained at magnifications of 40,000 and 20,000 \times for membranes A, B, and C, respectively. Obviously, different surface SEM images are observed and these differences are clearer from membrane A to C. For example, the surface morphology of membranes A and B was very smoother and denser, and no obvious pores can be found [cf. Fig. 4(a,b)]. However, a layered structure is detected in the surface of membrane C [cf. Fig. 4(c)], which indicates that phase-separated structure has occurred when the PEG content increased to some extent. This finding suggests that increasing PEG content makes poor distribution of filler in the membrane matrix and lower PEG content conduces to produce uniform filler distribution. Such difference in the surface morphology of these hybrid membranes may affect their PV separation performances.

The differences in membrane surface can be ascribed to an increase in the crosslinking degree in the hybrid network, resulting in these membranes become much tighter. Furthermore, the decrease in the compatibility of PEG and silica segments should be responsible for the phase-separated structure in membrane C because of the formation of PAMTMS-rich domains. Meanwhile, such phase-separated structure will play an important role in the separation of organic–organic compounds and benefit the permeation of active organic ingredients across the hybrid membranes. This can be used to explain the higher flux and separation factor of membrane C as discussed in PV measurements (cf. Figs. 5 and 6, hereinafter).

Pervaporation measurements

Effects of IPA content in feed on PV properties

Commonly, for PV separation of organic mixtures, understanding the dependence of feed concentration

TABLE V
Arrhenius Activation Energy Data

Sample	E_p (J/mol)	J_0	R^2
A	431.156	76.638	0.842
B	257.397	120.263	0.841
C	344.039	134.598	0.956

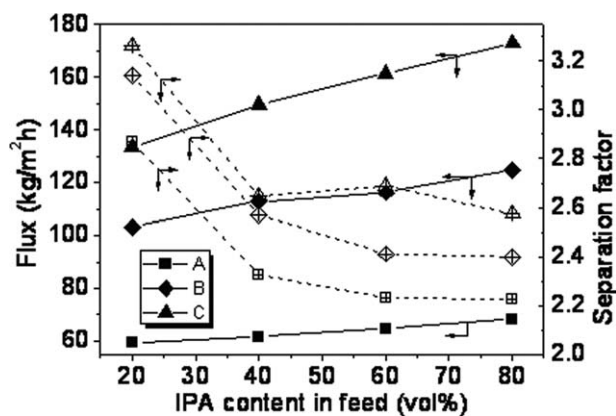


Figure 5 Effects of IPA content in feed on the permeation flux and separation factor of membranes A, B, and C; A (Square), B (Diamond), and C (UpTriangle) at 30°C.

on the permeation flux and separation factor is of vital importance.¹⁸ The effects of IPA content in feed on the permeation flux and separation factor of membranes A, B, and C are presented Figure 5.

Clearly, for different membranes A, B, and C, the permeation flux and separation factor follow such order as: membrane C > membrane B > membrane A, i.e., increases with the elevated PEG content in hybrid membranes. Whereas, for individual membrane, the permeation flux all enhances and the separation factor all decreases with an increase in the IPA content in feed, revealing an typical trade-off effect.²⁵

To explain the above trend, the following dominating factors need to be taken into consideration: (1) an increase in the concentration difference of IPA in feed will create larger penetrating effect and facilitate the permeation of IPA across the membranes, resulting in a promotion in permeation flux, (2) the increasing IPA content in feed will make polymer chains become more flexible, and the transport of IPA across the membranes become easier,¹⁸ which also bring on an increase in permeation flux, (3) an increase in PEG content in the hybrid membrane will enhance the affinity of membrane for IPA and phase-separated structure in membrane surface (cf. Fig. 4), leading to an increase in the diffusion rate of IPA across the membrane, accordingly increases the permeation flux. Meanwhile, the permeation of benzene also becomes easier because of the increasing flexibility of membrane when IPA content in feed increases. These combined effects on permeation flux of IPA and benzene will affect the separation factor.

Effects of feed temperature on PV properties

It is well accepted that feed temperature can significantly affect the permeation flux and separation fac-

tor of a pervaporation membrane.¹⁸ To examine the effects of feed temperature on the permeation flux and separation factor, the dependence of feed temperature on PV properties of membranes A, B, and C in 60 vol % IPA content in feed was determined and showed in Figure 6.

It can be noted that for individual membrane, the permeation flux of membranes A, B, and C is independent of feed temperature when the experimental error is considered; suggesting that feed temperature has little impact on the transport of IPA. This finding demonstrates that feed temperature does not affect the mobility of polymer chains and the change of free volume.^{10,18} However, it can also be noted that the separation factor increases remarkably with the elevated feed temperature, implying that the improvement of membrane selectivity. The reason can be ascribed to the formation of hybrid network, and an increase in the crosslinking degree of hybrid matrix, resulting in the creation of intimate or dense molecular structure as observed in FE-SEM images (cf. Fig. 4). Moreover, the permeation rate of IPA across the hybrid membranes becomes more rapid than that of benzene at high temperature, which will also be responsible for such trend.

Furthermore, by comparison the permeation flux across membranes A, B, and C, it can be found that it increases with the elevated PEG content in these hybrid membranes within the range of 30–60°C. The reason can be ascribed to their structural differences in membranes A, B, and C (cf. Fig. 4) and discussed above.

Permeation activation energy

Understanding permeation activation energy (E_p) can enhance the further investigation of PV separation properties of a hybrid membrane. Some researchers used permeation flux against feed

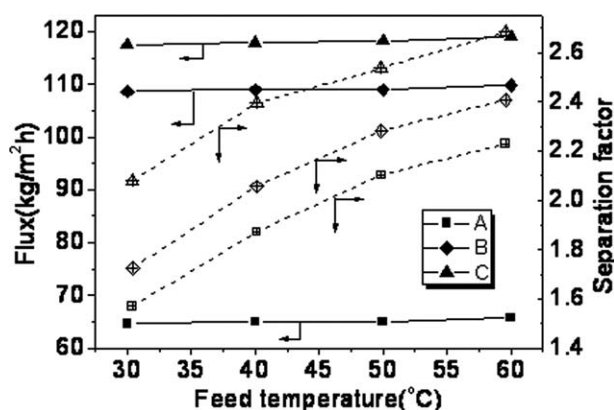


Figure 6 Effects of feed temperature on the permeation flux and separation factor of membranes A, B, and C; A (■), B (◆), and C (▲) in 60 vol % IPA content in feed.

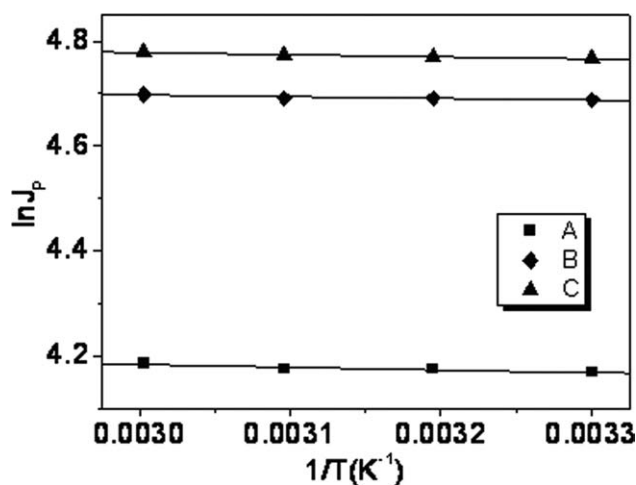


Figure 7 Dependence of $\ln J_P$ on $1/T$ of membranes A, B, and C in 60 vol % IPA content in feed.

temperature to predict the PV separation properties of membranes and have achieved fruitful results.^{9,18} Presently, E_P (J/mol) can be calculated based on the following Arrhenius-type expression¹⁸:

$$J_P = J_0 \exp\left(-\frac{E_P}{RT}\right) \quad (3a)$$

or,

$$\ln J_P = -\frac{E_P}{RT} + \ln J_0 \quad (3b)$$

where J_P is the permeation flux of component ($\text{g}/\text{m}^2 \text{h}$), J_0 is the pre-exponential factor, R is the gas constant ($8.314 \text{ J}/\text{mol K}$), and T is the solution temperature (K). E_P and J_0 can be calculated from the slope and intercept of the linear plot according to $\ln J_P$ vs. $1/T$ (cf. Fig. 7). The calculated results are presented in Table V.

As shown in Figure 7, it can be seen that the experimental data indicate well linear relationship [the linear regression coefficient (R^2) values are in the range of 0.84–0.95], implying permeation activation energy is dependent on the feed temperature.

By comparison the Arrhenius activation energy data in Table V, it can be noted that the permeation activation energy decreases from membrane A to C and indicate an opposite change trend with T_g and T_c , suggesting the influence of additive PEG on membrane property. The affinity of PEG for IPA might be responsible for such trend. Moreover, it should be pointed out that membrane B reveals the minimum E_P value among membranes A, B, and C; which can be ascribed to its lower T_g and T_c values as presented in DSC curves (cf. Fig. 3, hereinbefore). Based on the lower E_P values, it can be deduced that these hybrid membranes have potential applications

in the PV separation of IPA from isopropanol/benzene mixtures.

CONCLUSIONS

To separate isopropanol/benzene binary mixtures via PV technique, pervaporation hybrid membranes with different PEG content were prepared from PEG and PAMTMS using sol-gel reaction. FTIR spectra, DSC measurement, and FE-SEM images were used to characterize these membrane properties. PV experiments were used to evaluate their separation performances; meanwhile, the effects of IPA content in feed and feed temperature on both the permeation flux and separation factor are investigated. It is demonstrated that these hybrid membranes are IPA selective for isopropanol/benzene mixtures. The permeation flux increases and the separation factor decreases with an increase in IPA content in feed at 30°C . Meanwhile, the separation factor increases with the elevated feed temperature at 60 vol % IPA content in feed solution. Furthermore, it is found that feed temperature has no obvious impact on the permeation flux, suggesting that feed temperature has little contribution to the PV properties of the prepared hybrid membranes. These findings are meaningful in the pervaporation separation of isopropanol/benzene binary mixtures.

It should be emphasized that the separation factor of these hybrid membranes is not high. Consequently, for their industrial application, further work is required to optimize the preparation process of these hybrid membranes so as to improve the separation factor and permeation flux. It is hoped that this problem will be resolved with the preparation of high-flux hybrid membranes.

The authors specially thank Mr. Chenliang HAN for the analytical support of FE-SEM images.

References

1. Qiu, W.; Kosuri, M.; Zhou, F.; Koros, W. J. *J Membr Sci* 2009, 327, 96.
2. Zhang, Q. G.; Liu, Q. L.; Chen, Y.; Wu, J. Y.; Zhu, A. M. *Chem Eng Sci* 2009, 64, 334.
3. Lang, W. Z.; Tong, W.; Xu, Z. L. *J Appl Polym Sci* 2008, 108, 370.
4. Hyder, M. N.; Huang, R. Y. M.; Chen, P. *J Membr Sci* 2009, 326, 343.
5. Bakhshi, A.; Mohammadi, T.; Aroujalian, A. *J Appl Polym Sci* 2008, 107, 1777.
6. Peng, F. B.; Lu, L. Y.; Sun, H. L.; Pan, F. S.; Jiang, Z. Y. *Ind Eng Chem Res* 2007, 46, 2544.
7. Ohshima, T.; Matsumoto, M.; Miyata, T.; Uragami, T. *Macromol Chem Phys* 2005, 206, 473.
8. Zhang, Q. G.; Liu, Q. L.; Jiang, Z. Y.; Chen, Y. *J Membr Sci* 2007, 287, 237.
9. Liu, L.; Jiang, Z. Y.; Pan, F. S. *J Appl Polym Sci* 2006, 101, 90.

10. Wang, L. H.; Tian, Y.; Ding, H. Y.; Li, J. D. *Eur Polym J* 2006, 42, 2921.
11. Kulkarni, S. S.; Kittur, A. A.; Aralaguppi, M. I.; Kariduraganavar, M. Y. *J Appl Polym Sci* 2004, 94, 1304.
12. Dean, J. A. *Lange's Handbook of Chemistry*; 15th Ed.; McGraw-Hill: New York, 1998.
13. Xu, T. W. *J Membr Sci* 2005, 263, 1.
14. Wu, C. M.; Xu, T. W.; Gong, M.; Yang, W. H. *J Membr Sci* 2004, 247, 111.
15. Wu, C. M.; Xu, T. W.; Yang, W. H. *J Membr Sci* 2003, 224, 117.
16. Luo, J. Y.; Wu, C. M.; Wu, Y. H.; Xu, T. W. *J Membr Sci* 2010, 347, 240.
17. Liu, J. S.; Xu, T. W.; Fu, Y. X. *J Membr Sci* 2005, 252, 165.
18. Chen, J. H.; Liu, Q. L.; Zhu, A. M.; Fang, J.; Zhang, Q. G. *J Membr Sci* 2008, 308, 171.
19. Innocenzi, P.; Brusatin, G.; Guglielmi, M.; Bertani, R. *Chem Mater* 1999, 11, 1672.
20. Wu, C. M.; Xu, T. W.; Yang, W. H. *J Membr Sci* 2003, 216, 269.
21. Rodríguez-Lugo, V.; Sanchez Hernández, J.; Arellano-Jimenez, Ma. J.; Hernández-Tejeda, P. H.; Recillas-Gispert, S. *Microsc Microanal* 2005, 11, 516.
22. Patwardhan, S. V.; Taori, V. P.; Hassan, M.; Agashe, N. R.; Franklin, J. E.; Beaucage, G.; Mark, J. E. *Eur Polym J* 2006, 42, 167.
23. Chen, W.; Feng, H.; He, D.; Ye, C. *J Appl Polym Sci* 1998, 67, 139.
24. Yu, X.; Nagarajan, M. R.; Li, C.; Gibson, P. E.; Cooper, S. L. *J Polym Sci Part B: Polym Phys* 1986, 24, 2681.
25. Peters, T. A.; Benes, N. E.; Keurentjes, J. T. F. *J Membr Sci* 2008, 311, 7.